



Cite this: *New J. Chem.*, 2017, 41, 7849

Received 12th April 2017,  
Accepted 4th July 2017

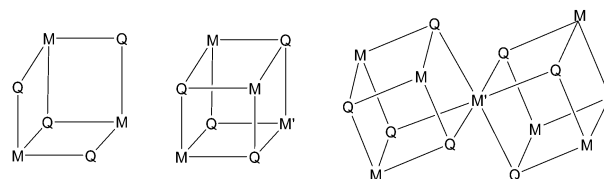
DOI: 10.1039/c7nj01217a

rsc.li/njc

# Synthesis, molecular structures and EPR spectra of the paramagnetic cuboidal clusters with $\text{Mo}_3\text{S}_4\text{Ga}$ cores†

Pavel A. Petrov,<sup>ab</sup> Dmitry Yu. Naumov,<sup>a</sup> Taisiya S. Sukhikh,<sup>ab</sup> Sergey N. Konchenko,<sup>ab</sup> Carlos J. Gómez-García<sup>c</sup> and Rosa Llusar<sup>bd</sup> \*<sup>d</sup>

Electron precise  $[\text{Mo}_3(\mu_3\text{-S})(\mu\text{-S})_3(\text{diphos})_3\text{Br}_3]\text{Br}$  (diphos = dppe, dmpe) incomplete cuboidal clusters with six cluster skeletal electrons (CSE) were converted into paramagnetic cuboidal  $[\text{Mo}_3(\text{GaBr})(\mu_3\text{-S})_4(\text{diphos})_3\text{Br}_3]$  clusters by treatment with elemental Ga. The new heterobimetallic complexes with nine CSE possess a doublet ground state with the unpaired electron density delocalized over the three molybdenum atoms.



Scheme 1

The cubane-type  $\text{M}_4\text{S}_4$  unit is known for many metals including molybdenum and gallium.<sup>1</sup> Heterobimetallic  $\text{Mo}_3\text{M}'\text{S}_4$  cores are also known for both transition and post-transition metals and they are synthesized by incorporating the  $\text{M}'$  metal into a preformed  $\text{Mo}_3(\mu_3\text{-S})(\mu\text{-S})_3$  fragment, presented in Scheme 1. The most common sources of this  $\text{Mo}_3\text{S}_4$  fragment are the  $[\text{Mo}_3\text{S}_4(\text{H}_2\text{O})_9]^{4+}$  aqua ion, the  $[\text{Mo}_3\text{S}_4(\eta^5\text{-Cp}^\#)_3]^+$  ( $\text{Cp}^\# = \text{C}_5\text{H}_5$ ,  $\text{C}_5\text{H}_4\text{Me}$ , or  $\text{C}_5\text{Me}_5$ ) cations and the  $[\text{Mo}_3\text{S}_4(\text{diphosphane})_3\text{X}_3]^+$  ( $\text{X} = \text{halogen}$ ) complexes.<sup>2</sup> However, to date post-transition group 13–15 metals have only been incorporated into the  $[\text{Mo}_3\text{S}_4(\text{H}_2\text{O})_9]^{4+}$  ion to afford single cubanes as well as corner-shared double cubane structures (see Scheme 1, metal–metal bonds are omitted for clarity).<sup>3</sup> Interconversion between single and double cubane structures is initiated by a redox change. In the case of gallium, only single cubane structures have been characterized to date. The  $[\text{Mo}_3\text{GaS}_4(\text{H}_2\text{O})_{12}]^{5+}$  and  $[\text{Mo}_3\text{GaS}_4(\text{H}_2\text{O})_{12}]^{6+}$  complexes have been prepared by a reaction of the  $[\text{Mo}_3\text{S}_4(\text{H}_2\text{O})_9]^{4+}$

aqua ion with gallium metal in 0.5 and 2 M  $\text{HCl}(\text{aq})$ , respectively.<sup>4a</sup> Reaction of the  $\text{Mo}_3\text{S}_4^{4+}$  aqua ion with  $\text{Ga}^{3+}$  in the presence of  $\text{NaBH}_4$  as the reducing agent exclusively affords the  $[\text{Mo}_3\text{GaS}_4(\text{H}_2\text{O})_{12}]^{5+}$  cluster cation.<sup>4b</sup>

Our groups have extensively investigated the chemistry of diphosphane-substituted  $\text{Mo}_3\text{S}_4$  complexes and we have isolated a series of heterobimetallic single cubane  $\text{Mo}_3\text{M}'\text{S}_4$  derivatives for  $\text{M}' = \text{Fe}$ ,<sup>5</sup>  $\text{Co}$ ,<sup>6</sup>  $\text{Ni}$ <sup>7</sup> and  $\text{Cu}$ .<sup>8</sup> In an attempt to extend this chemistry to post-transition metals, we reacted the cationic  $[\text{Mo}_3\text{S}_4(\text{dppe})_3\text{Br}_3]^+$  cluster (dppe = 1,2-bis(diphenylphosphino)ethane) with an excess of gallium metal resulting in the one-electron reduction of the cluster core, to afford an unusual paramagnetic  $[\text{Mo}_3\text{S}_4(\text{dppe})_3\text{Br}_3]$  complex.<sup>9</sup> In a similar way, its tungsten congener  $[\text{W}_3\text{S}_4(\text{dppe})_3\text{Br}_3]$  has also been isolated.<sup>10</sup> These  $[\text{M}_3\text{S}_4(\text{dppe})_3\text{Br}_3]$  paramagnetic clusters with seven cluster skeletal electrons (CSE) constitute rare examples of  $\text{Mo}_3\text{Q}_4$  complexes, which are, in general, electron precise with 6 CSE for the formation of three metal–metal bonds. It is noteworthy that the reaction of the analogous  $[\text{Mo}_3\text{Se}_4(\text{dppe})_3\text{Br}_3]^+$  cluster selenide with gallium results in a core transformation to afford a bicapped  $\text{Mo}_3\text{Se}_5$  cluster complex.<sup>11</sup> These results evidence the unique reactivity of gallium and prompted us to further study its incorporation into the  $\text{Mo}_3\text{S}_4$  core in order to obtain diphosphane  $\text{Mo}_3\text{GaS}_4$  derivatives.

As highlighted in the introduction, metallic gallium can serve as one-electron reductant transforming the 6 CSE electron precise  $\text{Mo}_3\text{S}_4$  diphosphane cluster cation to its neutral 7 CSE congener. When the reaction between  $[\text{Mo}_3\text{S}_4(\text{diphosphane})_3\text{Br}_3]\text{Br}$  and gallium is carried out under rigorous air-free conditions for a

<sup>a</sup> Nikolaev Institute of Inorganic Chemistry SB RAS, Lavrentiev Av. 3, 630090 Novosibirsk, Russian Federation. E-mail: panah@niic.nsc.ru; Fax: +7 (383) 316 9489; Tel: +7 (383) 316 5845

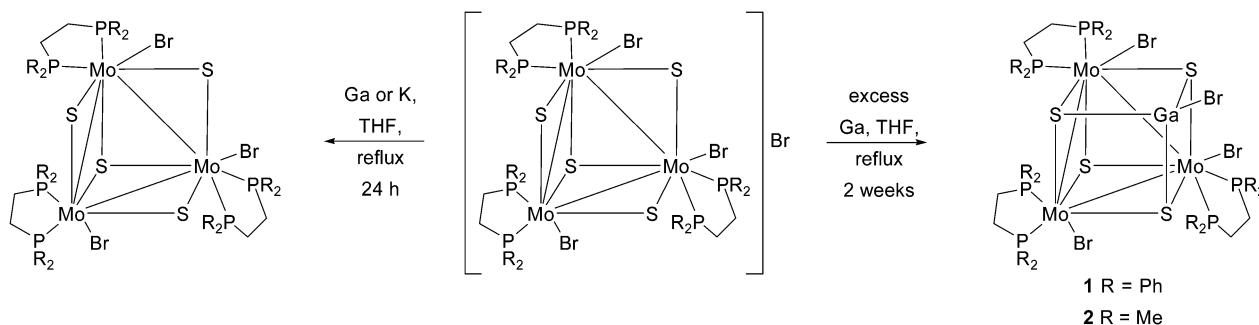
<sup>b</sup> Novosibirsk State University, Pirogov St. 2, 630090 Novosibirsk, Russian Federation

<sup>c</sup> Instituto de Ciencia Molecular (ICMol), C/Catedrático José Beltrán, 2, Universidad de Valencia, 46100 Paterna (Valencia), Spain

<sup>d</sup> Departament de Química Física i Analítica, Universitat Jaume I, Av. Sos Baynat s/n, 12071 Castelló, Spain. E-mail: rosa.llusar@uji.es; Fax: +34 964 728066; Tel: +34 964 728086

† Electronic supplementary information (ESI) available: Experimental details, structural data, magnetic susceptibility data and EPR spectra. CCDC 1542006 and 1542007. For ESI and crystallographic data in CIF or other electronic format see DOI: 10.1039/c7nj01217a





Scheme 2

reaction time of two weeks, as presented in Scheme 2, cubane type clusters  $[\text{Mo}_3\text{GaS}_4(\text{dppe})_3\text{Br}_4]$  (**1**) and  $[\text{Mo}_3\text{GaS}_4(\text{dmpe})_3\text{Br}_4]$  (**2**) are formed, and can be isolated in moderate yields (see Scheme 2). It is reasonable to assume that the reduced  $\text{Mo}_3\text{S}_4(\text{diphosphane})_3\text{Br}_3$  species with 7 CSE are formed first along with low valent gallium halides, resulting from the oxidation of gallium metal. Then, formal addition of a  $\text{Ga}^{\text{I}}\text{Br}$  vertex to the trimetallic 7 CSE cluster produces **1** and **2**, both containing 9 CSE. The other two  $\text{Mo}_3\text{Ga}$  clusters reported to date  $[\text{Mo}_3\text{GaS}_4(\text{H}_2\text{O})_{12}]^{5+}$  and  $[\text{Mo}_3\text{GaS}_4(\text{H}_2\text{O})_{12}]^{6+}$  contain 8 and 7 CSE, respectively. Incidentally, the reaction of  $[\text{Mo}_3\text{S}_4(\text{dppe})_3\text{Cl}_3]\text{Cl}$  or  $[\text{W}_3\text{S}_4(\text{dppe})_3\text{Br}_3]\text{Br}$  with an excess of gallium metal always stops at the reduction stage and without evidence for  $\text{Mo}_3\text{GaS}_4$  or  $\text{W}_3\text{GaS}_4$  species. Moreover, we were unable to isolate the reduced 7 CSE  $\text{Mo}_3\text{S}_4(\text{dmpe})_3\text{Br}_3$  derivative with a less bulkier and more basic diphosphane than dppe, and the reaction of  $[\text{Mo}_3\text{S}_4(\text{dmpe})_3\text{Br}_3]\text{Br}$  with gallium invariably yielded **2** as the only isolable product.

The crystal structures of **1**·4.5THF and **2**·THF were determined by single crystal X-ray diffraction, and both complexes share identical structural features.<sup>‡</sup> An ORTEP drawing of the molecular structure of **2** is presented in Fig. 1. Both structures consist of discrete molecules of **1** and **2** with a central  $\text{Mo}_3\text{Ga}$  core.

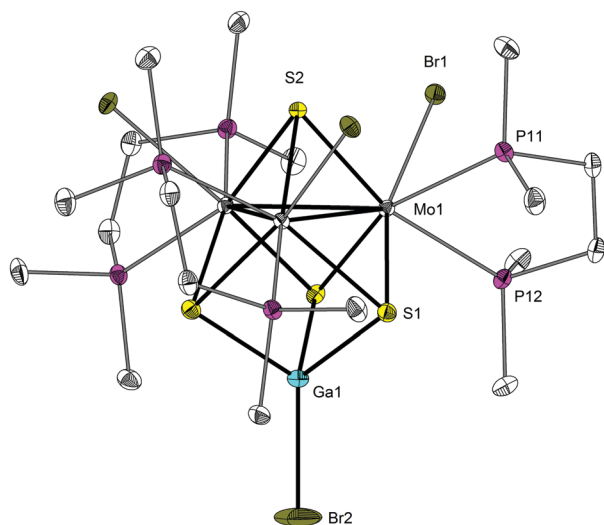


Fig. 1 ORTEP drawing of **2** with 50% thermal ellipsoids and the atom-numbering scheme. Hydrogen atoms are omitted for clarity.

Compound **2** crystallizes in the trigonal  $R3c$  space group with the S4, Br4 and Ga1 atoms lying on a  $C_3$  axis with a unique Mo–Mo bond distance of 2.7784(6) Å and a S4–Ga1–Br4 angle of 180°. The  $\text{Mo}_3$  triangle in **1** shows small deviations from a three-fold symmetry (ESI,<sup>†</sup> Fig. S1). The Mo–Mo bond lengths in **1** fall within the range 2.7756(7)–2.8132(7) Å and the Br atom coordinated to Ga is deviated from the central S4–Ga1 axis ( $\angle \text{S4–Ga1–Br4}$  equals 175.52(5)°). Table 1 lists the most relevant bond distances of compounds **1** and **2** together with those reported for the closely related  $\text{Mo}_3\text{GaS}_4$  aqua clusters.

The average Mo–Mo bond distance in **1** of 2.795[18] Å is slightly shorter, by 0.03 Å, than that observed for its parent cluster  $[\text{Mo}_3\text{S}_4(\text{dppe})_3\text{Br}_3]$  with 7 CSE (2.82[3] Å).<sup>9</sup> The shortening of the Mo–Mo or W–W bond is typical when a post-transition element is added to the  $\text{M}_3\text{S}_4$  unit to form a heterocubane  $\text{M}_3\text{M}'\text{S}_4$  core. The opposite tendency is found for the Mo–Mo bond distances in  $[\text{Mo}_3\text{GaS}_4(\text{H}_2\text{O})_{12}]^{5+}$  (2.735[8] Å) and  $[\text{Mo}_3\text{S}_4(\text{H}_2\text{O})_9]^{4+}$  (2.713[3] Å). There is an increase in the Mo–Mo bond lengths on going from  $[\text{Mo}_3\text{GaS}_4(\text{H}_2\text{O})_{12}]^{6+}$  with 7 CSE to  $[\text{Mo}_3\text{GaS}_4(\text{H}_2\text{O})_{12}]^{5+}$  with 8 CSE and to **1** and **2** with 9 CSE. This increase in Mo–Mo bond lengths is accompanied by a significant decrease of ca. 0.2–0.3 Å in the Mo–Ga bond distances. The coordination environment of molybdenum in **1** and **2** is similar to that of their trimetallic  $[\text{Mo}_3\text{S}_4(\text{diphosphane})_3\text{X}_3]$  precursors. The gallium atom in **1** and **2** has tetrahedral coordination in contrast to the octahedral environment found for the  $\text{Mo}_3\text{GaS}_4$  aqua clusters.

Compounds **1** and **2** with an odd number of electrons are expected to be paramagnetic. At 300 K the product of the molar magnetic susceptibility times the temperature,  $\chi_m T$ , for **1** (see Fig. S2, ESI<sup>†</sup>) and **2** equals ca. 0.34 emu K mol<sup>−1</sup> in both compounds (near the expected value of 0.375 for one unpaired electron) and remains almost constant when the temperature is decreased, as expected for a paramagnetic system. The isothermal magnetization at 2 K (Fig. S3, ESI<sup>†</sup>) shows a saturation value close to 1  $\mu_B$ , confirming the presence of a single unpaired electron in both compounds. The Q-band solid state EPR spectra of solid samples of **1** and **2** are very similar (Fig. 2 and Fig. S4, ESI,<sup>†</sup> respectively) with only one signal whose intensity increases upon decreasing the temperature. The signal presents axial anisotropy in both compounds although in compound **2** it shows a rhombic anisotropy at very low temperatures. This fact may be due to the larger distortions in the Mo coordination environment in **2**.

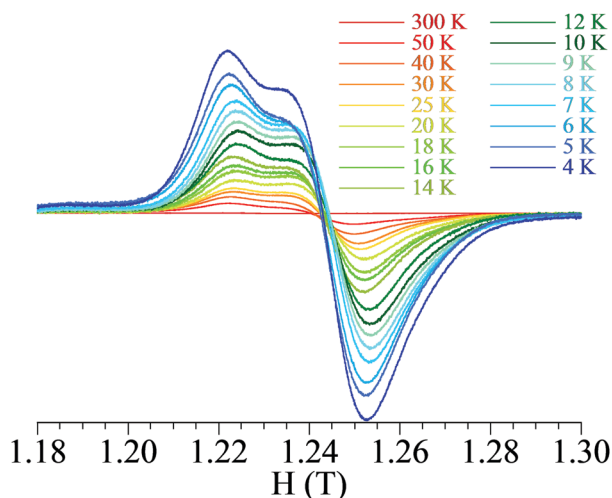


**Table 1** Selected average bond distances (Å) for cluster complexes with a  $\text{Mo}_3\text{GaS}_4$  core<sup>a</sup>

Distance	1	2	$[\text{Mo}_3\text{GaS}_4(\text{H}_2\text{O})_{12}]^{5+}$	$[\text{Mo}_3\text{GaS}_4(\text{H}_2\text{O})_{12}]^{6+}$
Mo–Mo	2.795[18]	2.7784(6)	2.713[3]	2.679[6]
Mo–Ga	3.33[4]	3.2704(8)	3.52[2]	3.60[2]
Mo–( $\mu_3\text{-S}$ ) <sup>b</sup>	2.354[2]	2.3624(13)	2.32[2]	2.332[3]
Mo–( $\mu_3\text{-S}$ ) <sup>c</sup>	2.399[5] <sup>d</sup>	2.4296(11) <sup>d</sup>	2.303[5]	2.335[4]
	2.391[14] <sup>e</sup>	2.3904(11) <sup>e</sup>		
Ga–S	2.34[2]	2.3099(12)	2.534[7]	2.50[1]
Ga–Br	2.3488(10)	2.3632(14)	—	—
Reference	This work	This work	<b>4a</b>	<b>4a</b>

<sup>a</sup> Standard deviations are given in parentheses; standard deviations for averaged values are given in square brackets. <sup>b</sup>  $\mu_3\text{-S}$  capping  $\text{Mo}_3$  face.

<sup>c</sup>  $\mu_3\text{-S}$  capping  $\text{Mo}_2\text{Ga}$  face. <sup>d</sup> Distance *trans* to the Mo–P bond. <sup>e</sup> Distance *trans* to the Mo–Br bond.

**Fig. 2** Q-band solid state EPR spectrum of **1** at different temperatures.

Thus, **2** has a more rhombic coordination environment with three different Mo–S bond distances (2.3624(13), 2.3904(11) and 2.4296(11) Å, Table 1), whereas in **1** we observed a more axial distortion since two of these distances are almost identical (*ca.* 2.354, 2.391 and 2.399 Å). Both compounds show no hyperfine splitting at low temperature indicating that the unpaired electron is delocalized over the three metal centres. In contrast, the unpaired electron density in the trinuclear cluster  $[\text{Mo}_3\text{S}_4(\text{dppe})_3\text{Br}_3]$  is localized on one metal centre.<sup>9</sup>

The electronic structures calculated for  $[\text{Mo}_3\text{GaS}_4(\text{H}_2\text{O})_{12}]^{5+/6+}$  using the spin polarized discrete variational DV-X $\alpha$  method show that the orbitals in the HOMO–LUMO region mainly consist of Mo 4d atomic orbitals. These results are in agreement with the absence of hyperfine splitting at low temperatures in the registered EPR spectra.<sup>4</sup>

In conclusion, interaction of the trimetallic  $\text{Mo}_3\text{S}_4$  clusters with gallium causes transformation of the cluster core to afford the first examples of a  $\text{Mo}_3\text{Ga}(\mu_3\text{-S})_4$  cluster core coordinated by diphosphane ligands. The cubane-like core formation likely goes through the step of one electron reduction of the  $\text{Mo}_3\text{S}_4$  unit. The two isolated heterobimetallic cluster complexes possess an odd number of electrons resulting in an  $S = 1/2$  ground state. The latter was evidenced by means of magnetic susceptibility measurements and confirmed by EPR spectroscopy.

## Conflict of interest

There are no conflicts to declare.

## Acknowledgements

This work was supported by Russian Foundation for Basic Research (projects 12-03-33028 and 13-03-01088) and Russian Ministry of Education and Science and DAAD ('Michail Lomonosov' Scholarship for P. A. P.). The financial support of the Spanish Ministerio de Economía y Competitividad (Grant CTQ2015-65207-P) and Generalitat Valenciana (PrometeoII/2014/022) is gratefully acknowledged.

## Notes and references

‡ Crystal data for  $1 \cdot 4.5\text{C}_4\text{H}_8\text{O}$ :  $\text{C}_{96}\text{H}_{108}\text{Br}_4\text{GaMo}_3\text{O}_{4.5}\text{P}_6\text{S}_4$ ,  $M_r = 2325.15$ , monoclinic, space group  $C2/c$ ,  $a = 41.507(3)$  Å,  $b = 18.0564(11)$  Å,  $c = 28.275(2)$  Å,  $\alpha = 90^\circ$ ,  $\beta = 110.780(1)^\circ$ ,  $\gamma = 90^\circ$ ,  $V = 19813(2)$  Å<sup>3</sup>,  $Z = 8$ , 58 589 reflections measured, 20 131 independent reflections ( $R_{\text{int}} = 0.0430$ ). Final  $R$  indices:  $R_1 = 0.0654$  and  $wR_2 = 0.1833$  [ $I > 2\sigma(I)$ ];  $R_1 = 0.0942$  and  $wR_2 = 0.2083$  (all data). Largest diff. peak and hole: 3.245 and  $-1.006$  e Å<sup>-3</sup>. CCDC 1542006.† Crystal data for  $2 \cdot \text{C}_4\text{H}_8\text{O}$ :  $\text{C}_{22}\text{H}_{56}\text{Br}_4\text{GaMo}_3\text{OP}_6\text{S}_4$ ,  $M_r = 1327.91$ , trigonal, space group  $R3c$ ,  $a = b = 15.4061(2)$  Å,  $c = 31.5053(9)$  Å,  $\alpha = \beta = 90^\circ$ ,  $\gamma = 120^\circ$ ,  $V = 6475.9(2)$  Å<sup>3</sup>,  $Z = 6$ , 13 227 reflections measured, 2862 independent reflections ( $R_{\text{int}} = 0.0280$ ). Final  $R$  indices:  $R_1 = 0.0175$  and  $wR_2 = 0.0455$  [ $I > 2\sigma(I)$ ];  $R_1 = 0.0182$  and  $wR_2 = 0.0458$  (all data). Largest diff. peak and hole: 1.089 and  $-1.284$  e Å<sup>-3</sup>. CCDC 1542007.†

- (a) H. Seino and M. Hidai, *Chem. Sci.*, 2011, **2**, 847–857; (b) M. B. Power, J. W. Ziller and A. R. Barron, *Organometallics*, 1992, **11**, 2783–2790.
- R. Llusar and S. Uriel, *Eur. J. Inorg. Chem.*, 2003, 1271–1290.
- (a) R. Hernandez-Molina, M. N. Sokolov and A. G. Sykes, *Acc. Chem. Res.*, 2001, **34**, 223–230; (b) H. Akashi and T. Shibahara, *Inorg. Chem.*, 1989, **28**, 2906–2907; (c) G. Sakane and T. Shibahara, *Inorg. Chem.*, 1993, **32**, 777–778; (d) G. Sakane, Y. Yao and T. Shibahara, *Inorg. Chim. Acta*, 1994, **216**, 13–14; (e) J. E. Varey, G. J. Lamprecht, V. P. Fedin, A. Holder, W. Clegg, M. R. J. Elsegood and A. G. Sykes, *Inorg. Chem.*, 1996, **35**, 5525–5530; (f) R. Hernandez-Molina, A. J. Edwards, W. Clegg and A. G. Sykes, *Inorg. Chem.*, 1998, **37**, 2989–2994; (g) G. Sakane, K. Hashimoto, M. Takahashi, M. Takeda and T. Shibahara, *Inorg. Chem.*, 1998, **37**, 4231–4234; (h) Y. Qin, L. Wu, Z. Li, Y. Kang, Y. Tang and Y. Yao, *Chem. Lett.*, 2000,



- 950–951; (i) S.-F. Lu, J.-Q. Huang, Q.-J. Wu, X.-Y. Huang, R.-M. Yu, Y. Zheng and D.-X. Wu, *Inorg. Chim. Acta*, 1997, **261**, 201–209; (j) S.-F. Lu, J.-Q. Huang, R.-M. Yu, X.-Y. Huang, Q.-J. Wu, Y. Peng, J. Chen, Z.-X. Huang, Y. Zheng and D.-X. Wu, *Polyhedron*, 2001, **20**, 2339–2352.
- 4 (a) T. Shibahara, S. Kobayashi, N. Tsuji, G. Sakane and M. Fukuhara, *Inorg. Chem.*, 1997, **36**, 1702–1706; (b) R. Hernandez-Molina, V. P. Fedin, M. N. Sokolov, D. M. Satsel and A. G. Sykes, *Inorg. Chem.*, 1998, **37**, 4328–4334.
- 5 (a) A. G. Algarra, M. G. Basallote, M. J. Fernandez-Trujillo, R. Llusar, J. A. Pino-Chamorro, I. Sorribes and C. Vicent, *Dalton Trans.*, 2010, **39**, 3725–3735; (b) I. Sorribes, F. Lloret, J. C. Waerenborgh, V. Polo, R. Llusar and C. Vicent, *Inorg. Chem.*, 2012, **51**, 10512–10521.
- 6 M. Feliz, R. Llusar, S. Uriel, C. Vicent, E. Coronado and C. J. Gómez-García, *Chem. – Eur. J.*, 2004, **10**, 4308–4614.
- 7 M. Feliz, R. Llusar, S. Uriel, C. Vicent, M. Brorson and K. Herbst, *Polyhedron*, 2005, **24**, 1212–1220.
- 8 M. Feliz, E. Guillamón, R. Llusar, S.-E. Stiriba, J. Pérez-Prieto and M. Barberis, *Chem. – Eur. J.*, 2006, 1486–1492.
- 9 P. A. Petrov, D. Yu. Naumov, R. Llusar, C. J. Gómez-García, V. Polo and S. N. Konchenko, *Dalton Trans.*, 2012, **41**, 14031–14034.
- 10 P. A. Petrov, A. I. Smolentsev and S. N. Konchenko, *Russ. J. Coord. Chem.*, 2013, **39**, 510–513.
- 11 P. A. Petrov, M. R. Ryzhikov, A. V. Virovets, S. N. Konchenko, C. J. Gómez-García and R. Llusar, *Polyhedron*, 2014, **81**, 6–10.

